Simulated rockburst experiment—an overview

by T.O. Hagan*, A.M. Milev*, S.M. Spottiswoode*, M.W. Hildyard*, M. Grodner*, A.J. Rorke†, G.J. Finnie‡, N. Reddy*, A.T. Haile*, K.B. Le Bron*, and D.M. Grave*

Synopsis

A simulated rockburst experiment was conducted underground at a deep level gold mine. This was done by means of a large explosion detonated in solid rock close to a tunnel sidewall. The resultant shake-out damage is typical of that associated with a small seismic event in close proximity to a tunnel that is subjected to the estimated field stress, as in this case, of 50 MPa.

The experiment involved:

- **the design of a blast to mimic a seismic source**
- **seismic monitoring using a dense seismic array**
- **high speed video filming**
- **a study of rock mass conditions (fractures, joints, rock strength etc.) before and after the simulation using mapping and ground penetrating radar**
- **special investigations to evaluate the mechanism and the magnitude of the damage**
- **a study of support behaviour under excessive dynamic loading.**

Introduction

Designing and effectively supporting excavations in seismically active mines needs a substantially improved understanding of rockburst damage mechanisms and excavation site response to seismicity.

The current level of rockburst studies is limited by the lack of strong ground motion data recorded in the immediate vicinity of large seismic sources. Jesenak, *et al.*[4] commented: 'Many investigators have developed direct relationships between damage levels and ground motion parameters. However, difficulties resulting from highly subjective assessment criteria and incomplete or questionable peak ground motion data severely limit the applicability of these relationships. This limitation will only be overcome when high quality strong ground motion data has been collected and properly analysed'.

The severity of rockburst damage often varies greatly over small distances. One panel in a longwall may be severely damaged, while an adjacent panel (perhaps even closer to the focus of the seismic event) is unscathed. Both Spottiswoode, *et al.*[1] and Milev, *et al.*[2] found that ground motion measured at points about 1 m apart on the stope hangingwall showed variations of up to a factor of five in kinetic energy.

Durrheim, *et al.*[3] found that seismic damage to underground excavations depends upon three main factors namely the seismic source mechanism, the rockburst damage mechanism and the site response. The source mechanism refers to phenomena associated with the failure of the rocks, often at pre-existing weaknesses such as faults or dykes, which release seismic energy. When the seismic waves radiated by the source interact with an excavation, the motion of the skin may vary greatly due to numerous factors such as the geometry of the cavity, effect of support systems, and the degree of fracturing. This variability is termed the site response. In situations where the hangingwall or sidewall collapses or the face bursts, the term 'rockburst damage mechanism' is used to refer to these phenomena. It is believed that a better understanding of these phenomena will enable those areas, which have a high potential for sustaining rockburst damage to be identified, and provide design criteria for support systems. In some cases part of the excavation lies within the near field of the seismic source and so the source and the damage mechanism cannot be really separated.

This paper summarizes the results obtained from the simulation of a rockburst by means of a large underground explosion in the vicinity of the wall of a mine tunnel. The research, undertaken by Hagan, *et al.*[5], formed

* *CSIR: Division of Mining Technology, Johannesburg, South Africa.*

† *Bulk Mining Explosives (Pty) Ltd, Johannesburg, South Africa.*

‡ *Department of Chemical Engineering, Technikon Northern Gauteng.*

 SA ISSN 0038–223X/3.00 + 0.00. Paper received Feb. 2001; revised paper received Jul. 2001.

part of a larger project aimed at improving mine worker safety through an improved understanding of the mine excavation site response to seismicity. The following stages were involved in the experiment: numerical modelling (Hildyard and Milev[6]) to mimic a seismic source by means of a blast; the installation of a micro-seismic array; near and far field seismic monitoring (Milev, *et al.*[7]); high speed video filming to derive the ejection velocities (Rorke and Milev[14]) a study of rock mass conditions (fractures, joints, rock strength etc.) before and after the blast to estimate the extent and type of damage brought about by strong ground motion (Reddy and Spottiswoode[8] and Grodner[9]) and evaluation of the support performance under dynamic loading (Haile and Le Bron[10]).

Test site and instrumentation

The simulation was conducted in an unused tunnel and access crosscut on Kopanang Mine in the Klerksdorp region. The excavations are 1600 m below surface in fairly weak argillaceous quartzites (UCS = 130 MPa).

Figure 1 shows the site geometry. Mining of the Vaal Reef (on the same level) was in progress at the time of the experiment. The mining was some 100 m NNW of the site to the west of the fault shown. This is a normal fault dipping east with a throw of 100 m.

MINSIM modelling showed a theoretical field stress of 50 MPa at the site. The mining, 100 m to the NNW, brought this up from the theoretical virgin stress of 42 MPa.

Bedding in the quartzites ranges in thickness from 5 to 50 cm and the beds are often separated by thin argillaceous partings. The dip ranges between 30° and 50° with the steeper dips closer to the fault, probably as a result of drag during the faulting progress.

'Bow wave' stress fractures formed during the development of the tunnel. They define angles of up to 20° to the sidewall. Dips are steep, ranging between 85° and 90°. As with the bedding they occur all along the tunnel. Their orientation with respect to the tunnel is illustrated in only one small zone in Figure 1.

Five 102 mm blastholes were drilled from a cubby in the access crosscut in a direction roughly parallel with the tunnel. An attempt was made to drill the holes in a vertical plane with the collars about 50 cm apart. The exact hole positions

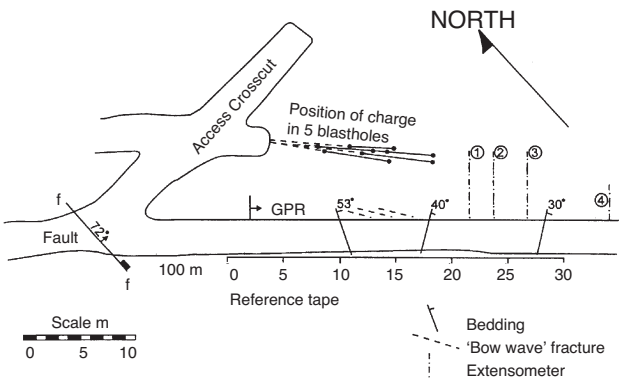

Figure 1—Geometry of the simulated rockburst experiment site

were surveyed relative to the tunnel sidewall. Figure 1 shows the charged portions of the holes on plan. These are never closer than 5 m to the tunnel sidewall to ensure that gas expansion into the tunnel wall would not occur, otherwise this could have added to the damage caused by the shockwaves from the blast.

Each hole was charged with ANFO using a compressed air loader. The holes were stemmed with quick-setting cement cartridges. The blasts were initiated using electronic detonators, 10g/m detonating cord with two Powergel 816 emulsion cartridges in each hole acting as primers. The primer position was located 1 m into the charge from the stemming end.

The detonating cord lengths were measured to achieve initiation in all holes within a 0.3 ms time window. Initiation progressed at 0.07 ms intervals between holes from bottom to top.

The holes were primed at the collar end of the charge to minimize the deleterious influence on the explosive of the detonating cord initiation lines and to give a more controlled time history of the blast. These primer positions, however, prevented the measurement of explosive detonation velocity. The total mass of ANFO explosive detonated was 261,5 kg.

Two shock type accelerometers were installed on the blasting wall opposite to the blast charges in the area of maximum expected damage. Ground Motion Monitors comprising 32 geophones were installed along the tunnel. The transducers were placed on the sidewalls, the hangingwall and the footwall. Vertical, horizontal and tri-axial geophone boats, installed on the skin and into a borehole, were used to provide maximum coverage.

The sidewall was whitewashed before the experiment to allow easy identification of subsequent damage due to the simulated rockburst.

Source design and calibration

Extensive numerical modelling, using a finite difference WAVE (Cundall[17], Hildyard and Milev[6,15]) together with empirical equations generally employed in blasting practice (Parnes[18], Daenhke[19], Kouzniak and Rossmanith[20], Rossmanith *et al.*[21] and Uenishi *et al.*[22]) was used to design the source of the simulated rockburst. The following parameters were considered:

- source—tunnel geometry. Chosen to prevent direct damage from the gas expansion
- expected peak particle velocities and their distribution on the tunnel wall
- position of the monitoring equipment to provide maximum seismic coverage.

However, the preliminary numerical modelling and the use of empirical equations for the calculation of peak particle velocities on the sidewall gave large variations in their values and position. It was therefore decided to perform a small calibration blast. This, together with further numerical modelling, enabled the estimation of maximum peak particle velocities as a function of charge mass and number of holes.

Near field effects

Observed damage

Figure 2 is a photograph of the damage to the sidewall as a result of the simulated rockburst. The volume of blocks

Figure 2—Damage on the tunnel sidewall induced by the simulated rockburst

ejected per metre of the wall was used to quantify the degree of damage on the blasting wall. Two areas of damage were clearly observed namely an area of relatively high intensity damage located opposite the charges and an area of relatively low intensity damage further along the tunnel. Except for some loose rocks that had fallen from the hangingwall, no damage was observed on the hangingwall, footwall and the sidewall opposite to the blast.

Reddy and Spottiswoode[8] showed that the shape of ejected blocks was determined by the pre-existing bedding separations and stress fractures. A visual inspection indicated that no direct gas expansion was involved in the ejection of the rocks.

The degree of fracturing was commensurate with the estimated field stress of 50 MPa. Tunnels that are, or have been, subjected to field stresses well in excess of 50 MPa show tunnel-paralled fracturing and massive sidewall movement that is exacerbated by strong ground motion.

Reddy and Spottiswoode[8] conclude that the damage to the sidewall was therefore mostly a shake-out, as the expected field stress of 50 MPa was insufficient to cause additional damage. In addition, because the tunnel was not surrounded by a thick fractured zone, opportunities for dilation were limited.

After the blast all shotholes were examined using a borehole video camera. The examination showed that a large vertical crack formed connecting all boreholes. The crack had a 'wavy' shape with the opening decreasing from the collar of the hole towards the toe. Photographs of the crack are shown in Figure 3.

Numerical model vs. damage

Figure 4 compares the modelled maximum induced tensile stresses for the sidewall of the tunnel with recorded damage (Hildyard and Milev[15]). Regions marked 'H' and 'L' indicate areas where the relatively high and low intensity damage was observed. Induced vertical stress in σ_{zz} is concentrated opposite the blastholes (maximum 25 MPa) with a maximum of 10 MPa ahead of the blast. The induced tensile stress in σ_{yy} is also high opposite the blastholes (maximum 25 MPa), but there is a second highly tensile region ahead of the blast on the edge of the low intensity damage zone. This becomes less marked for lower frequency sources.

The above stresses could lead to tunnel-normal fracturing, but should be seen in the context of the total stress state. The tunnel was at a depth of 1600 m, giving estimates for the virgin stress of 42 MPa vertical and 21.5 MPa horizontal.

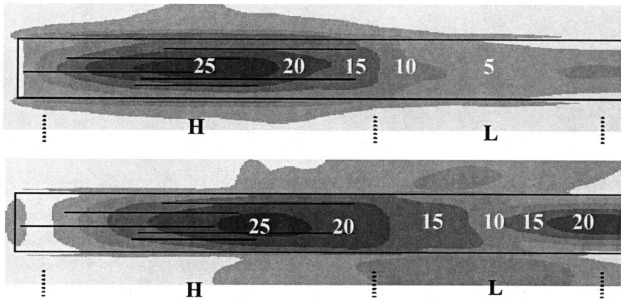

Figure 4—Distribution of maximum induced tensile stress (in MPa) at the tunnel sidewall. Upper figure shows the σ_{zz} vertical stress distribution and bottom figure shows the σ_{yy} distribution parallel to the sidewall. Positions 'H' and 'L' show the regions where relatively high and low intensity damage were reported

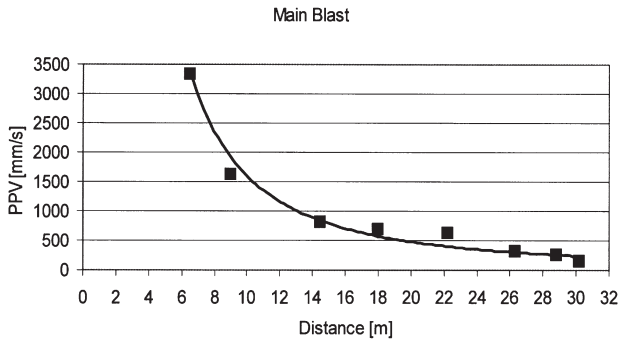

Figure 5—Attenuation of the peak particle velocities as measured along the tunnel wall

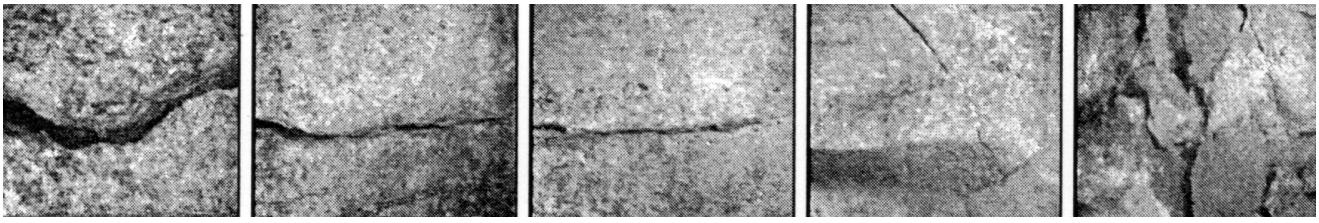

Figure 3—A series of photographs along the roof of one of the boreholes taken after the blast

Peak particle velocities measured on the tunnel sidewall

Two accelerometers were located in the area of damage. The first accelerometer, located in the area of high density damage, was ejected with a piece of rock at a peak particle velocity of 3.3 m/s. The second accelerometer, located in the area of low intensity damage, remained on the wall at a peak particle velocity of 1.6 m/s.

Accelerometer and geophone readings allowed for the estimation of the attenuation of peak particle velocity down the tunnel wall moving away from the blast (Figure 5).

The attenuation of maximum velocities from the calibration blast $Y_{(R)}$ as a function of distance from the blast R was derived as:

$$Y_{(R)} = C\frac{1}{R^{1.7}} \qquad [1]$$

where C is a constant proportional to the mass of the charge. Similar values were reported by Ouchterlony *et al.*[16].

Ejection velocities from high speed video filming

A high-speed camera was used to film the tunnel sidewall and to measure the rock fragment ejection distances. A speed of 200 frames per second was set in accordance with the lighting conditions in the tunnel. This frame rate provided a time resolution of 5 ms per frame.

Nine orange balls were positioned on the tunnel wall closest to the charges. They were located in three vertically aligned sets of three balls each. They were placed 1 m apart vertically and sets were placed 2.5 m apart horizontally. The purpose of the balls was to provide locality information and scaling for the high-speed film.

The first vertical set was located directly opposite the centre of gravity of the explosive charges. The second set was located in line with the end of the charged holes and the third set was located 2,5 m further on down the tunnel.

Fragment velocities were measured by tracking individual fragment positions through space at intervals of 10 frames (equal to 50 ms) at a time. This was done manually by measuring distances on the projected image and converting these to actual distances using the target ball positions for scaling.

The equation used to convert from the projected image distances to actual distances was:

$$Distance\ in\ mm\ = \left(8.457 \times Projected\ image\ distance\ in\ pixels\right) / \cos 14° \qquad [2]$$

The factor 8.457 converts from image pixels to actual distances in mm and was obtained by measuring the projected image distance between two marker balls. The angle of the camera to the blasting wall was 14°. The correction factor was applied because it was assumed that the rock fragments were ejected at right angles to the tunnel wall.

The fragments showed a random behaviour for times greater than 100 ms perhaps due to excessive camera vibration after that time. All data points above 100 ms were therefore excluded. Calculated ejection velocities are listed in Table I.

The area where the ejection velocities were measured corresponds approximately to the position of the second accelerometer located in the area of low intensity damage. The peak particle velocity of 1.6 m/s measured at this point agrees reasonably well with the range of the ejection velocities.

Far field monitoring and comparison with mine tremors

Many stations making up the Klerksdorp regional seismic network recorded the simulated rockburst. The local magnitude was estimated as M_L = 1.3.

There are significant physical differences in the process of a seismic wave generated by blasting and by dislocation source types. In view of this it was important to analyse and compare the structure of the blast seismogram and some of its source parameters recorded in the far field with those generated by dislocation type mining-induced tremors located in adjacent areas.

The waveforms recorded from the simulated rockburst experiment show well-developed body wave groups on all components. However, the portion of the energy radiated into the P-waves is greater than the portion of the energy radiated into the S-waves when compared to dislocation type seismic sources. Figure 6 compares the energy radiated into P- and S- waves for the blast and for 14 mining-induced seismic events, which located in the same region of the mine.

An important characteristic of seismic source dynamics is the stress drop, or the difference between the state of stress before and after the rupture. Stress drop can be represented as a plot of log E versus log M_O (where E is the radiated seismic energy and M_O is the scalar seismic moment). A blasting source would normally generate a significantly smaller stress drop. Figure 7 shows that the seismic energy radiated from the blast in fact does create a smaller seismic

Table I

Ejection velocities obtained from high speed filming

Fragment #	Ejection velocity (m/s)
Ball	V_B = 1.075
Fragment 2	V_2 = 0.846
Fragment 3	V_3 = 0.705
Fragment 4	V_4 = 0.652
Fragment 5	V_5 = 0.740
Fragment 6	V_6 = 1.813
Fragment 7	V_7 = 2.467

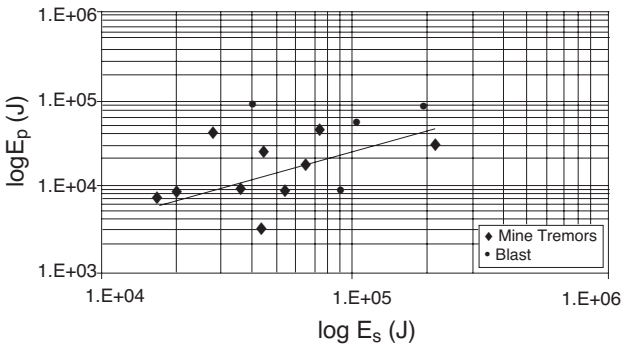

Figure 6—Energy radiated in P- waves versus energy radiated in S-waves for the blast and for 14 mine-induced seismic events located in the same region of the mine

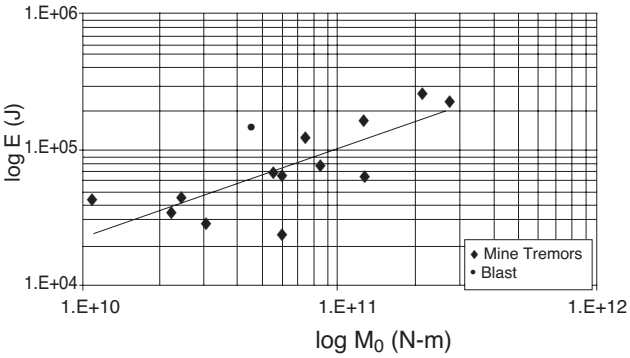

Figure 7—Energy versus moment for the blast and 14 mine-induced seismic events located in the same region of the mine

moment than the dislocation type seismic events. The simulated rockburst characteristics have a higher energy to moment ratio and significantly different P-waves.

Support behaviour

The existing support system of the tunnel consisted of rock bolt reinforcement units and mesh and lacing fabric support. The fabric support system used to contain the rock was not active at the site. Therefore, without significantly disturbing the integrity of the support system, the mesh and lace was removed from the sidewall, before the simulated rockburst experiment, to allow ejection of the rock blocks.

The behaviour of the rock bolts during the simulated rockburst experiment indicated a limited interaction between the rock bolt and the rock mass at the boundary of the excavation. Peak particle velocities of 3.3 m/s measured in the area of relatively high intensity damage had severely damaged the rock mass between the support units without failure of a single rock bolt reinforcement unit indicating that they were not loaded by the full tributary volume of rock assigned to each bolt.

The survival of these relatively stiff rock bolt units under excessive seismic loading has also been observed at numerous rockburst sites by Haile[11], Hagan, *et al.*[12], and Haile and Hagan[13].

An array of geophones was set up between rockbolt units on the tunnel sidewall enabling the measurement of peak particle velocity with increasing distance from the rock bolt unit. It was shown that the units only reinforce and confine the rockmass effectively in their immediate vicinity, and that there is an increased potential for block ejection and rockmass unravelling with increased rock bolt spacing.

Rockburst damage occurred at this site only where the PPV, measured at the skin of the tunnel, exceeded 0.7 m/s. This understanding would allow the design of rock bolt spacing, for this site, to prevent rockmass unravelling for an anticipated dynamic loading condition based on the derived relationship between rock bolt spacing and PPV amplification.

The relationship between measured rockburst damage with distance from the rock bolt reinforcement and level of dynamic loading (PPV) was clearly illustrated. It is this potentially unstable rockmass volume that will define the demand on, and thus the capacity of, typical mesh and lace fabric support systems.

Ground penetrating radar results

Ground penetrating radar (GPR) was used by Grodner[9] to determine the position and nature of the fractures in the tunnel sidewall in the area of the simulated rockburst experiment. By comparing the radar scans acquired before and after the simulated rockburst (Figure 8 vs. Figure 9 respectively), it was possible to determine which fractures were reactivated and where new fractures were formed. Mining-induced fractures that formed during the development of the tunnel were re-activated as indicated by their increased reflectance on the radar scans. In addition, several new fractures developed in the area of, and parallel to, the blastholes. In other words GPR showed how and where the fracturing changed and therefore contributed to the understanding of the mechanisms of damage associated with the simulated rockburst.

Conclusions

Important findings:

- The 5 m distance of the blast holes from the tunnel

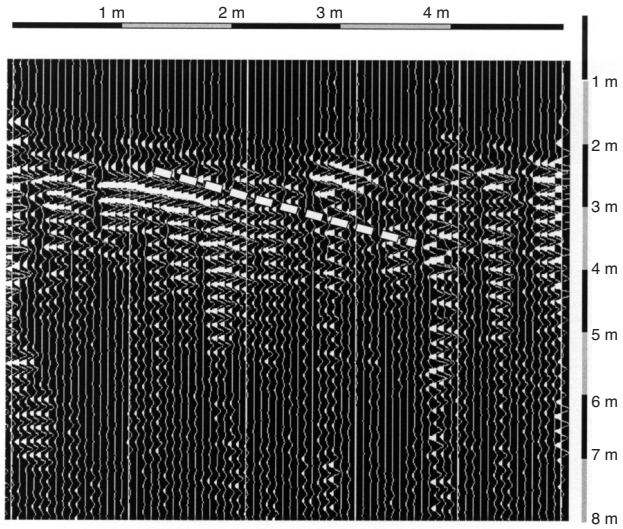

Figure 8—Part of one of the GPR scans (before the blast) penetrating 8 m into the tunnel wall. Oblique mining-induced 'bow wave' fractures are evident. Direction of tunnel development is from right to left

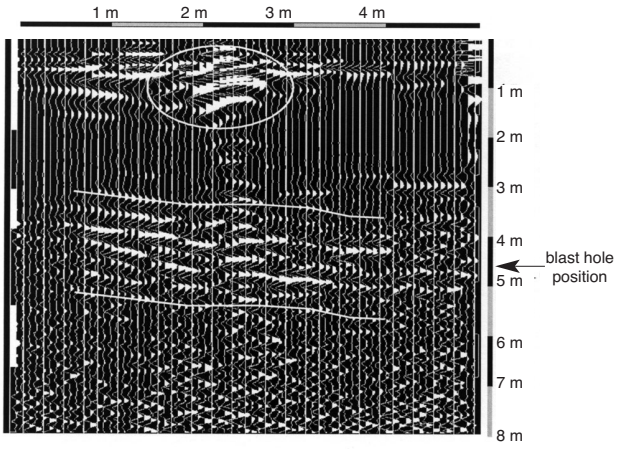

Figure 9—A GPR scan of the same area as Figure 8 but taken after the blast. The scan shows a change in the fractures close to the tunnel wall and the development of new fractures in the vicinity of the blastholes

wall ensured that no gas pressure was directly involved in damaging the wall of the tunnel

- Two areas of damage were identified on the blasting wall: (i) an area with relatively high intensity damage where ground velocities of 3.3 m/s were recorded by an accelerometer ejected with a block of rock, and (ii) an area with relatively low intensity damage where ground velocities of 1.6 m/s were recorded by an accelerometer which remained on the tunnel wall
- Rockburst damage occurred on the tunnel wall where the PPV exceeded 0.7 m/s
- High speed filming revealed rock fragments being ejected from the wall at velocities in the range of 0.7 m/s to 2.5 m/s. The measurements were taken in the area of low intensity damage
- The attenuation of maximum velocities for the main blast as a function of distance from the blast R was found to follow the law of $1/R^{1.7}$, in the near field (6 m to 30 m)
- The simulated rockburst was recorded by the Vaal River Operations regional seismic network with a magnitude estimated at $M_L = 1.3$.
- Fractures, together with the natural bedding planes and the fractures formed during the development of the tunnel, determined the shape of blocks ejected from the wall at the time of simulated rockburst
- It was possible, using GPR, to determine changes in fracturing brought about as a result of the simulated rockburst
- The experiment offered an opportunity to study the influence that rock bolts have on the rockmass when it is subjected to dynamic loading. This improved understanding of the interaction between rock bolts, and a discontinuous rockmass under dynamic loading conditions, should assist in improving support design
- Rock bolt support of the tunnel had the effect of reducing the peak particle velocities and damage to the wall in their immediate vicinity only. No failure of the support units was observed indicating that they were not loaded by the full tributary volume of rock assigned to each unit
- The results highlight the potential for the use of numerical models to gain greater insight into the interaction of seismic waves with fractured rock.

Acknowledgements

This work was part of the research programme supported by the Safety in Mines Research Advisory Committee (SIMRAC) under the project GAP 530. We would like to thank the management, production and rock engineering staff of the Kopanang Mine for their outstanding assistance and co-operation at various stages of the experiment.

References

1. Spottiswoode, S.M., Durrheim, R.J., Vakalisa, B., and Milev, A.M. Influence of fracturing and support on the site response in deep tabular stopes, *Proc. 1st SARES*, R.G. Gürtunca and T.O. Hagan (Editors), Johannesburg, 1997. pp. 62–68.
2. Milev, A.M., Spottiswoode, S.M., and Stewart, R.D. Dynamic response of the rock surrounding deep level mining excavations. *Proc. 9th ISRM*, G. Vonille and P. Berset (Editors), Paris'99, 1999. pp. 1109–1114.
3. Durrheim, R.J., Milev, A.M., Spottiswoode, S.M., and Vakalisa, B. Improvement of worker safety through the investigation of the site response to rockbursts. *SIMRAC Final Project Report GAP 201*, Pretoria: Department of Minerals and Energy, 1997. 530 pp.
4. Jesenak, P., Kaiser, P.K., and Brummer, R.K. Rockburst damage potential assessment. *Proc. 3rd Int. Symp. on Rockbursts and Seismicity in Mines*: Rotterdam, Balkema. 1993. pp. 81–86.
5. Hagan, T.O., Milev, A.M., Spottiswoode, S.M., Vakalisa, B., and Reddy, N. Improvement of worker safety through the investigation of the site response to rockbursts. *SIMRAC Final Project Report GAP 530*, Pretoria: Department of Minerals and Energy, 1998. 147 pp.
6. Hildyard, M.W. and Milev, A.M. Simulated rockburst experiment: Development of a numerical model for seismic wave propagation from the blast, forward analysis. J. of South African Inst. of Mining and Metallurgy, submitted for publication. 2001.
7. Milev, A.M., Spottiswoode, S.M., Rorke, A.J., and Finnie, G.J. Seismic monitoring of a simulated rockburst on a wall of an underground tunnel. J. of South African Inst. of Mining and Metallurgy, submitted for publication. 2001.
8. Reddy, N., and Spottiswoode, S.M. The influence of geology on a simulated rockburst experiment. J. of South African Inst. of Mining and Metallurgy, submitted for publication. 2001.
9. Grodner, M. Using Ground Penetrating Radar to quantify changes in the fracture pattern associated with a simulated rockburst experiment. J. of South African Inst. of Mining and Metallurgy, submitted for publication. 2001.
10. Haile, A.T. and Le Bron, K.B. Simulated rockburst experiment—evaluation of rock bolt reinforcement performance. J. of South African Inst. of Mining and Metallurgy, submitted for publication. 2001.
11. Haile, A.T. A mechanistic evaluation and design of tunnel support systems for deep level South African mines. Ph.D. thesis, Mechanical Engineering Dept., University of Natal, South Africa, 1999. 302 pp.
12. Hagan, T.O., Durrheim, R.J., Roberts, M.K.C., and Haile, A.T. Rockburst investigations in South African mines. *Proc. 9th ISRM Congress*. G. Vonille and P. Berset (Editors). Paris, France. 1999. pp. 1809–1094.
13. Haile, A.T. and Hagan, T.O. Tunnel design implications from a study of rockburst investigations. T.R. Stacey, R.G. Stimson and J.L. Stimson (Editors) *Proc. AITES-ITA 2000*, World Tunnel Congress, Durban, South Africa. 2000. pp. 185 –190.
14. Rorke, A.J and Milev, A.M. Near Field Vibration Monitoring and Associated Rock Damage, *FRAGBLAST 1999*, Johannesburg, South African Institute of Mining and Metallurgy. 1999.
15. Hildyard, M.W. and Milev, A.M. Simulated rockburst experiment: Numerical back analysis of seismic wave interaction with the tunnel. J. of South African Inst. of Mining and Metallurgy, submitted for publication. 2001.
16. Ouchterlony, S.N., Nyberg, U., and Deng, J. Monitoring of large open cut rounds by VOD, PPV and gas pressure measurements. *Fragblast International Journal of Blasting and Fragmentation*, vol. 1, no. 1, 1997. pp. 3–25.
17. Cundall, P.A. 'Theoretical basis of the program WAVE'. Unpublished internal report, *COMRO* (now Miningtek, CSIR, South Africa), 1992, pp. 1–12.
18. Parnes, R. Response of an infinite elastic medium to travelling loads in a cylindrical bore. *J. Appl. Mech*., 1969, vol. 36, pp. 51–58.
19. Daehnke, A. Stress wave and fracture propagation in rock. Ph.D. thesis, Vienna University of Technology, 1997. 408 pp.
20. Kouzniak, N. and Rossmanith, H.P. Supersonic detonation in rock mass—Analytical solutions and validation of numerical models—Part I: Stress analysis. *FRAGBLAST Int. J. of Blasting and Fragmentation*, 1998, vol. 2, # 4. pp. 449–486.
21. Rossmanith, H.P., Uenishi, K., and Kouziak, N. Blast wave propagation in rock mass—Part I: monolithic medium. *FRAGBLAST Int. J. of Blasting and Fragmentation* 1, 1997. pp. 317–359.
22. Uenishi, K. and Rossmanith, H.P. Blast wave propagation in rock mass—Part II: layered media. *FRAGBLAST Int. J. of Blasting and Fragmentation* 2, 1998. pp. 39–77. ◆